



Cite this: *Green Chem.*, 2025, **27**, 6430

Received 13th March 2025,
Accepted 14th May 2025

DOI: 10.1039/d5gc01293g

rsc.li/greenchem

A microbial factory for bio-indigo synthesis: demonstration of sustainable denim dyeing†

Matteo Planchestainer,[‡] Lin Chen,[§] Tsvetan Kardashliev,[‡] Sven Panke[‡] and Martin Held[‡]*

Biotechnological production using genetically engineered bacteria has the potential to enable environmentally friendly manufacturing of indigo without toxic intermediates or by-products, as in the case of traditional chemical processes. The shikimate and tryptophan pathways of *Escherichia coli* were engineered to supply a high level of the key intermediate indole, which was then converted to indigo by a naphthalene dioxygenase. The final strain yielded up to 12 g L⁻¹ of indigo dye under optimised cultivation conditions. The indigo was then purified using a sustainable process and used for dyeing of cotton fibers.

Green foundation

1. The engineered *E. coli* strain converts a renewable carbon source into indigo dye through a fully biological process. This eliminates hazardous chemical synthesis steps, lowers the operating temperature (reducing energy consumption), and avoids toxic byproducts. This work showcases how synthetic biology and biocatalysis can be used to produce bulk chemicals through fully sustainable and alternative routes.
2. Microbially produced indigo was synthesized at 30 °C using a glucose-based feedstock. The resulting dye demonstrated comparable dyeing properties to chemically synthesized indigo. However, no detectable amounts of toxic compounds, which are typically found in chemically produced indigo, were present in our biologically derived product.
3. Further optimization of the *E. coli* strain to enhance indigo yield would improve process efficiency, reducing water and feedstock consumption. Additionally, improvements in downstream processing (DSP) and implementing water recycling strategies, would further enhance sustainability and minimize resource use.

Introduction

Indigo is the key dye to produce denim textiles, conferring the characteristic colour of blue jeans. It is known for its distinctive chemical characteristics, such as poor water solubility, intense dyeing capability, and conferring the unique blue-shaded “wash-out” characteristic of dyed denim.

Originally, indigo was isolated from the leaves of the *Indigofera tinctoria* plant.^{1,2} In 1901, the Heumann–Pfleger synthesis¹ was developed, starting from aniline and chloroacetic acid to yield indigo (Fig. 1A) in four steps. This achievement marks a milestone in the history of chemistry and enabled the further scaling of indigo production to the current level of over 80 000 tons per year.² However, the high output comes at a

price, as carcinogenic residues (mainly aniline or *N*-methylaniline) necessitate costly post-synthetic purification and product polishing.^{3,4} Furthermore, since fossil carbon is used as a starting material, all emissions generated over the entire indigo life cycle contribute to greenhouse gas emissions and global warming.⁵

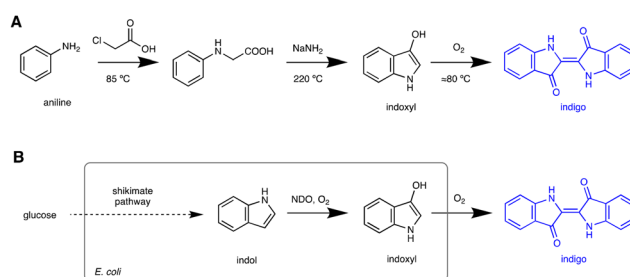


Fig. 1 Indigo synthesis. Scheme of the chemical Heumann–Pfleger (A) and the microbial indigo synthesis (B). While the chemical synthesis starts from fossil derived and carcinogenic aniline, the biosynthesis employed renewable glucose isolated from plants as a starting material (NDO, naphthalene dioxygenase).

BPL, D-BSSE, ETH Zurich, Klingelbergstrasse 48, Basel, CH-4056, Switzerland.

E-mail: matteo.planchestainer@fhmw.ch, martin.held@bsse.ethz.ch

† Electronic supplementary information (ESI) available. See DOI: <https://doi.org/10.1039/d5gc01293g>

‡ Current address: School of Life Sciences, FHNW, Hofackerstrasse 30, Murtens, CH-4132.

§ Current address: FGen AG/Ginkgo Bioworks Inc. Hochbergstrasse 60C, Basel, CH-4057.



Hence, there is interest in green indigo that is intrinsically free of toxic residues⁶ and ideally synthesised from non-fossil-based starting materials. Unfortunately, indigo produced by plants cannot satisfy the demand,⁷ but microbial synthesis from renewable carbon (e.g., glucose) has the potential to enable the step-change. Consequently, considerable efforts toward developing microbial routes for indigo production have been reported.² In the 1990s, Genencor LLC pioneered large scale indigo production by recombinant *Escherichia coli* cells.^{8,9} This strategy harnesses the cell's natural shikimate pathway for the synthesis of tryptophan (Trp) on the path to indole (Fig. S1†). Subsequently, a hydroxylase oxidizes indole to indoxyl, which then undergoes self-dimerization to form indigo in the presence of molecular oxygen (Fig. 1B). However, while some—though at least partially contradictory—information, including claims of indigo cultivation titres of 18 g L⁻¹, has been released by Genencor at that time, no details have been provided on downstream processing or product purification.

Similarly, other reported efforts have focused on developing improved microbial biocatalysts and fermentation processes but not on product isolation and purification. However, even though powerful metabolic engineering techniques (e.g., CRISPR/Cas9¹⁰) and bioinformatics tools¹¹ as for the first time used by us for recombinant indigo production have since been developed, advances in the field remain sizeable^{2,6} and the fermentation titres reported by Genencor have never been repeated by any other group (recent reports indicate a range of 1–2 g L⁻¹ (ref. 12 and 13)).

All reported efforts share the common goal of exploiting the anabolic sequence of Trp and its precursor shikimate biosynthesis. However, while Trp concentrations exceeding 50 g L⁻¹ in biotransformation reactions starting from glucose have been achieved,¹⁴ these achievements have not been yet transferred to engineering strains for indigo production.

Furthermore, several crucial aspects vital to industrial indigo production remain unexplored or are not available in the public domain. Notably, methods for the separation and refinement of indigo from the fermenter broth, as well as the fundamental question of whether indigo particles produced in bioreactors are predominantly located inside or outside bacterial cells, have not been reported yet. Curiously, there is also a notable absence of reports documenting the scaling and purification of microbially-catalysed processes for indigo production. The underlying reason for the meagre data is likely the poor solubility of indigo, which is nearly insoluble in water or any other protic or organic solvent. Consequently, extraction efforts followed by processes such as crystallization or diges-

tion are economically unfeasible. As a result, many methods routinely used in industrial biotechnology for product separation and purification cannot be applied. Indigo purification is therefore an intriguingly difficult task, which may provide the part of the reason why, to the best of our knowledge, no method for the preparation of microbially-produced indigo for textile dyeing has been reported so far.

We aim to address this knowledge gap by (I) constructing a state-of-the-art indigo-producing *E. coli* strain, integrating the latest knowledge from the literature on the engineering of the shikimate and Trp pathways required for the synthesis of the indigo precursor indole, (II) developing a DSP protocol for the isolation and purification of microbe-produced indigo using an efficient method amenable to scaling, and (III) testing the performance of the material for cotton fibre dyeing.

Results and discussion

Our original plan was to benchmark the strains from our program against the strain used by Genencor in the late 1990s.⁸ However, all our efforts to reproduce Genencor's reported work did not succeed as we could not reproduce the strain's genetic modifications (inactivation of *pykA* and *pykF*). Consequently, we focused initially on boosting flux through the shikimate and Trp synthesis pathways. This flux is constrained by various kinetic and genetic feedback regulations (Fig. S2†). Kinetic feedback inhibition are reported for AroG, the most active of the three housekeeping DAHP synthases, and TrpE, encoded in the *trpLEDCBA* operon for the conversion of chorismate to Trp. However, these inhibitory effects can be prevented by two amino acid exchanges (S180F for AroG¹⁵ and S40F for TrpE¹⁶) which were integrated by us. Moreover, both native promoters were substituted by the strong constitutive promoter J23119 thereby alleviating genetic feedback inhibitions. To elevate the genetic stability of the strain, all modifications were made directly on the genome relying on CRISPR/Cas9.¹⁷ The first two modifications, AroG^{S180F} and TrpE^{S40F}, were incorporated into BL21(DE3) and W3110 but their introduction into *E. coli* FM5 (the strain used by Genencor) failed for unexamined reasons. Next, Trp production was assessed as a proxy for the potential of the strain to deliver the indigo precursor indole. The results from shake flask experiments indicated 30% higher titre for BL21(DE3) J23119-*aroG*^{S180F} J23119-*trpE*^{S40F} (parental strain; G0b) compared to the W3110-based strain (G0w). Consequently, BL21 (DE3) was chosen for further strain engineering efforts (Table S1†).

The first indigo producing strain (generation 1; G1) was obtained by transformation of G0b with two plasmids harbouring three auxiliary enzymes: (i) the naphthalene dioxygenase from *Pseudomonas balearica* DSM 6083 (NDOb), for hydroxylation of indole to indoxyl. NDOb is homologue to NDO of *P. putida* used by Genencor, but with higher overall activity on indole when tested *in vivo* experiments (Table S2†); (ii) the isatin hydrolase (IH) from *P. putida*, for removal of isatin, a

†The data on the carbon feeding strategy seemed to be flawed. The stated conversion efficiency of glucose to indigo $Y_{\text{indigo/glucose}}$ is 0.61 mole_{indigo}/mole_{glucose} and therefore exceeds the theoretical possible conversion efficiency in *E. coli* $Y_{\text{indigo/glucose}} = 0.21$ mole_{indigo}/mole_{glucose} almost three-fold.^{34,35} Similarly, the reported conversion yields of tryptophan to indigo of 1 g_{indigo}/g_{tryptophan} (Fig. 2A at page 130 of Berry *et al.*⁸) exceed the maximum theoretical yield for this reaction of 0.64 g_{indigo}/g_{tryptophan} by more than 30%.



noxious overoxidation product of indoxyl,⁸ and (iii) the indole-3-glycerol phosphate lyase (BX1) from *Zea mays*¹⁸ that allows bypassing the wild-type TrpA-TrpB-TnaA cascade while reducing the liberation of indole before Trp formation (Fig. S1†). BX1, to best of our knowledge, has never been used in indigo but only in indole-producing *E. coli* strains. The resulting G1 strain allowed for production of indigo from glucose in 0.5 L fed-batch cultivations to levels of 0.8 g L⁻¹ (Table 1, Fig. S3†).

In the second generation, we targeted AroL, which catalyses the reaction of shikimate to shikimate 3-phosphate but whose expression is repressed by the two regulatory proteins TyrR and TrpR. To ensure permanent expression, the native promoter of the *aroL* gene was replaced with pL, a strong constitutive promoter.¹⁹ The resulting strain BL21(DE3) J23119-*aroG*^{S180F} J23119-*trpE*^{S40F} pL-*aroL* with the two plasmids encoding NDOb, IH, and BX1 (generation 2; G2) allowed producing up to 4.2 g L⁻¹ of indigo in fed-batch cultivations performed at 0.5 L scale (Table 1, Fig. S4†).

Strain G2 showed issues of process stability, as we recurring problems such as excessive foaming and sudden discontinuation of indigo production. When analysing possible reasons for this behaviour, we considered oxidative stress: *E. coli* does not natively express hydroxylases²⁰ such as NDOb. NDOb, in turn, is prone to form peroxides during catalysis. Hence, we suspected that at least a part of the observed problems could be due to oxidative stress.

As a countermeasure, we constitutively expressed the alkyl hydroperoxide reductase (*ahpC*) gene from the genome by changing the native to the constitutive promoter WG219.²¹ AhpC is known to efficiently reduce highly reactive noxious oxygen species (e.g. hydrogen peroxide or organic hydroperoxides) responsible for oxidative stress and reduced cell viability.²² The resulting strain G3 (*E. coli* BL21(DE3) J23119-*aroG*^{S180F} J23119-*trpE*^{S40F} pLtetR-*aroL* WG219-*ahpC* harbouring NDOb, IH, and BX1) yielded up to 7.3 g L⁻¹ of indigo (Table 1, and Fig. S5†) in fed-batch biotransformation performed at the 0.5 L lab-scale displaying improved reproducibility and less foaming during fermentation.

However, strain G3 accumulated acetate up to levels known to be toxic for *E. coli* (Fig. S5H†)²³ possibly due to the action of the phosphate acetyltransferase (Pta). Pta catalyses the conver-

sion of acetyl-CoA to acetyl phosphate, leading ultimately to the formation of ATP and acetate. To reduce acetate-formation, the mutation P69L was introduced into the *pta* gene thereby decreasing substrate affinity for acetyl-CoA and consequently the acetate formation rate.²⁴ It is worth noting that the attempt to knock out *pta* failed perhaps due to a strong impact on the ATP regeneration capacities of the G3 strain constitutively synthesizing amino acids intermediates known to pose a high metabolic burden.²⁵ However, the resulting strain G4 (*E. coli* BL21(DE3) J23119-*aroG*^{S180F} J23119-*trpE*^{S40F} pL-*aroL* WG219-*ahpC* *pta*^{P69L} harbouring NDOb, IH, and BX1) allowed production of indigo to levels of up to 8.3 g L⁻¹ (Table 1, Fig. S6†) in 0.5 L lab-scale bioreactors.

Other genomic modifications commonly employed in aromatic amino acid overproducing *E. coli* strains, such as boosting the erythrose 4-phosphate (E4P) and phosphoenolpyruvate (PEP) synthesis by *tktA* or *glpX* overexpression²⁶ or *pykA* or *pykF* downregulation,²⁷ were found to not further increase the indigo titre when introduced in G4 strain. Specifically, in all four cases, the obtained strain was phenotypically unstable (*i.e.*, very slow grow rate or no grow), which impeded further assessment.

We also analysed the broth for by-products possibly formed by strain G4. Intermediates indole, anthranilate, shikimate, chorismate, and indole-3-glycerol phosphate could not be detected either due to low concentrations or molecular instability. However, Tryptophan was found to accumulate to considerable concentrations (>7 g L⁻¹) (Fig. S6†) which prompted us to enhance the level of the housekeeping tryptophanase (TnaA) that catalyses its conversion to indole. Attempts to replace the native promoter *via* CRISP/Cas9 with a constitutive one failed for unknown reasons. However, increasing the gene copy number by transforming G4 with a third plasmid containing the *tnaA* gene under the control of the lac promoter, resulting in strain G5, led to an increased indigo production level of 12 g L⁻¹ (Fig. 2A, Table 1, Fig. S7†) in lab-scale 0.5 L fed-batch fermentations.

In parallel to optimising the strains, we developed a scalable and environmentally friendly protocol for indigo recovery and purification from cultivation broths such as those produced in fed-batch processes described above. We realized that

Table 1 Indigo producing strains. Final indigo concentrations reached in fed-batch cultivations of the indigo producing strains based on *E. coli* BL21(DE3) and equipped with auxiliary enzymes. Shown are the highest indigo titre achieved after optimization of fermentation protocols

| Strain code | <i>E. coli</i> BL21 (DE3) | Auxiliary enzymes | Max indigo titre (g L ⁻¹) | Indicative fermentation time (h) | Mean productivity (g h ⁻¹) |
|-------------|--|---------------------|---------------------------------------|----------------------------------|--|
| G1 | J23119- <i>aroG</i> ^{S180F} J23119- <i>trpE</i> ^{S40F} | IH, BX1, NDOb | 0.8 | 60 | 0.01 |
| G2 | J23119- <i>aroG</i> ^{S180F} J23119- <i>trpE</i> ^{S40F} pL- <i>aroL</i> | IH, BX1, NDOb | 4.2 | 65 | 0.06 |
| G3 | J23119- <i>aroG</i> ^{S180F} J23119- <i>trpE</i> ^{S40F} pL- <i>aroL</i> WG219- <i>ahpC</i> | IH, BX1, NDOb | 7.3 | 75 | 0.09 |
| G4 | J23119- <i>aroG</i> ^{S180F} J23119- <i>trpE</i> ^{S40F} pL- <i>aroL</i> WG219- <i>ahpC</i> <i>pta</i> ^{P69L} | IH, BX1, NDOb | 8.3 | 80 | 0.10 |
| G5 | J23119- <i>aroG</i> ^{S180F} J23119- <i>trpE</i> ^{S40F} pL- <i>aroL</i> WG219- <i>ahpC</i> <i>pta</i> ^{P69L} | IH, BX1, NDOb, TnaA | 12 | 100 | 0.12 |

NDOb: naphthalene dioxygenase from *P. balearica* DSM 6083; IH: isatin hydrolase from *P. putida*; BX1: indole-3-glycerol phosphate lyase from *Zea mays*; TnaA: tryptophanase from *E. coli*.



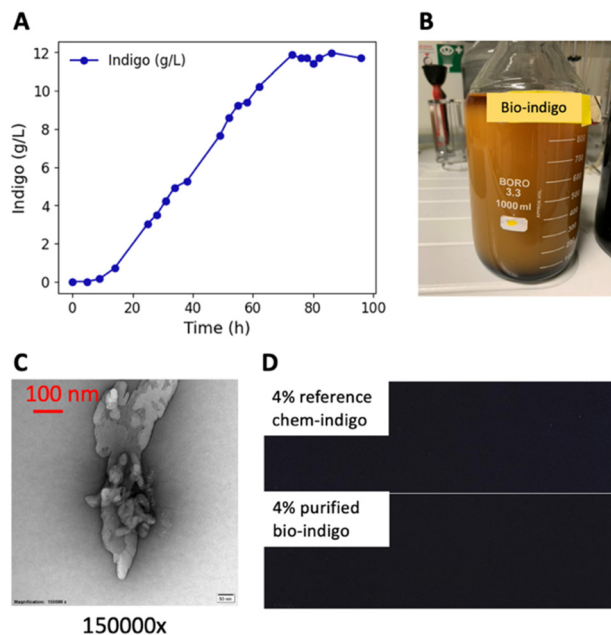


Fig. 2 Indigo production. (A) Indigo formation by strain G5 from glucose and ammonia; (B) image of the sedimentation process, showing the biomass (brown colouring of the aqueous phase) separated from the indigo (blue bottom layer) by sedimentation. Fermentation both of a 0.5 L-fermentations together with residual material removed from fermenter by rinsing with water (0.2–0.3 L); (C) electron microscopy image of a indigo particle post-purification with 0.5% citric acid and 121 °C treatment; (D) results of cotton fibres staining tests using indigo purified from cultivation broths (Table S3,† entry 6) and chemically synthesized industrial grade indigo.

with strain G5, biomass could be conveniently separated from the denser indigo crystals by sedimentation and decantation (Fig. 2B). Recovery and washing (three washing cycles with water) of the indigo found in the bottom phase resulted in a dye with a purity of approximately 70% when dried (Table S3,† entry 1). While this purity level is comparable to that obtained from processed plant-derived indigo, it falls short of chemically synthesized, industrial grade material (>95%).² Authenticity of indigo from fermentations was verified by its retention time and UV-Vis spectrum compared to chemically synthesized standards²⁸ after separation by HPLC (Fig. S8†). While results of elemental analysis of indigo after sedimentation and washing showed presence of sulphur and therefore indicates protein contaminations (Table S4†). Furthermore, electron microscopy revealed supramolecular structures formed by clusters adhering to the indigo particles (Fig. 2C, and S9†). Hence, we propose that the contaminants are likely to be cellular debris and proteins.

First, we attempted to further increase the purity of the indigo generated by microbial cultivation by reducing it to the water-soluble form, leucoindigo ("indigo-white").¹ We reasoned that in this way, insoluble cell debris and proteins can be removed by filtration or sedimentation prior to re-oxidation of leucoindigo to indigo and precipitation of the latter. The purity indeed increased to 91% (Table S3,† entry 2) but

the method generated a substantial amount of salts (up to 10 : 1 w/w of the indigo mass).²⁹ The high costs of the required chemicals together with the high salt load in the waste stream, indicate low economically and environmentally compatibility.

We hence decided to adapt a purification strategy for removal of biogenic impurities employing elevated temperature and acid catalysed hydrolysis previously reported by Hoffmann-La Roche AG for the purification of riboflavin (Vitamin B2)^{30,31} produced by *Bacillus subtilis*. An initial test indicated that indigo was remarkably stable at high temperature in presence of 5% sulfuric or citric acid. Indeed, upon the characteristic UV-Vis spectrum in DMSO was unchanged when heated in the acids over the temperature range (120 to 220 °C), indicating indigo stability under these conditions (Fig. S10†).

Next, we went through iterative cycles of protocol development and performed protein hydrolysis indigo from fermentations in 4–10% hydrochloric acid (HCl) or sulfuric acid (H₂SO₄) at temperatures ranging from 80 to 120 °C for between 10 and 120 minutes. The protocols yielded indigo of purities of up to 84% (Table S3,† entries 3 and 4). Next, we hypothesized that the mineral acids could be replaced by a more eco-friendly ones, like citric acid. After optimisation, a concentration of citric acid (0.5%) and thermal treatment of 20 min at 121 °C (30 psi) allowed to reproducibly prepare indigo from sedimented and washed indigo at a purity of 84% after drying (Table S3,† entry 6). As expected, all batches of indigo, regardless of the employed purification strategy, exhibited non-detectable levels (<6.3 ppm) of toxic anilines. In comparison, chemically synthesized indigo typically used for large scale denim dyeing (~95% quality) contains approximately 7000 ppm of amines (Table S5,† entry 1).

We conducted dyeing tests on cotton fabrics in collaboration with the Quality Control Laboratory at Archroma AG. A fixed amount of indigo was used to dye neutral-white cotton patches, and the resulting coloration was measured using a textile-grade UV-spectrophotometer (HunterLab Agera). The intensity and colour differences between the indigo samples were evaluated using the CMC ΔE (Delta E) method, developed by the Colour Measurement Committee,³² which is widely regarded as an industry standard for colour difference assessment (Table S3†). Indigo obtained by sedimentation and washing from fermentations (70% purity) showed a noticeably weak blue shade in the dyeing assay (Fig. S11A†). However, the negligible difference in dyeing intensity, both visually and by quantitative measurement (~100% staining intensity; Table S3,† entries 1–6), between chemically synthesized indigo (~95% purity; Fig. 2D) and thermally acid-treated indigo (84% purity) supports the suitability of the biologically produced material for industrial application (Fig. S11B–F†).

Experimental

Strain engineering

All the genomic modifications (promoter exchange, point mutations, gene insertions and deletions) were performed



with λ -red supported homologous recombination counter selected by CRISPR/Cas9 as developed by Jiang *et al.*¹⁷ Briefly, respective *E. coli* isolates were first transformed with the plasmid pCas (carrying the λ -red recombinase and Cas9) and then grown in the presence of 0.2% arabinose for recombinase-induction. The resulting strain was transformed with pTarget, which contained the DNA strand with the target modification and the sgRNA for counterselection. Successful gene modifications were identified after colony growth under selection pressure and subsequent confirmation by PCR and Sanger sequencing of the respective loci. All plasmids for gene editing were prepared by Gibson assembly methodology³³ and are listed in the ESI (Table S8†).

Fermentation

Bioreactor cultivation was carried out in Infors HT Minifors-2 (working volume 0.5 L) tabletop fermenters with flow disruptor inserts, equipped with acid and base pumps (aqueous H_2SO_4 10%/aqueous NH_4OH 20%) for pH control (pH probe Mettler Toledo InPro3100i/SG/225). Dissolved oxygen was measured using a sensor (Hamilton OxyFerm CIP) calibrated by sparging sterile complete cultivation medium with N_2 for 30 min (200 rpm, 0%) and air (21% oxygen, 30 min, 1000 rpm, sensor signal 100%). *E. coli* seed cultures of 25 mL in Luria-Bertani medium (LB, Difco™ LB Broth 25 g L^{-1}) in 250 mL glass flasks were inoculated by addition of a glycerol stock (0.2 mL) and then grown at 30 °C to the early stationary phase (OD_{600} of approx. 2 in *ca.* 10 h, 200 rpm, 2.5 cm amplitude). Bioreactors containing 380 mL of fermentation medium with 0.5% glucose (Table S6†) were inoculated to an OD_{600} of 0.1 by the seed cultures (*ca.* 20 mL, total cultivation volume of 400 mL). Aeration and stirring speed were automatically adjusted by the bioreactor's software to maintain the DOT at 20%. After about 24 hours the initially provided glucose was exhausted (DOT spiked over 20%) and the fed-batch phase was started immediately afterwards. Glucose was fed at a linearly increasing rate from 1 to 4 g $\text{L}^{-1} \text{h}^{-1}$ from a 60% solution (Table S7†) over 22 hours and then manually adjusted to avoid excessive accumulation of glucose to levels above 5 g L^{-1} (glucose was measured off-line every two hours). Typically, between 250 and 350 mL (equivalent to 200–300 g L^{-1} of glucose) were fed over 50–75 hours for a total fermentation time between 72 and 96 hours.

Quantification of components in the medium

Quantification of glucose and acetate in the cultivation medium was performed by RID-HPLC. After removing samples from liquid cultures, cellular activity was immediately quenched by the addition of H_2SO_4 to a final concentration of 10 mM. Particulates were removed by centrifugation (15 000g; 15 min), and an aliquot of the supernatant (5 μL) was analysed by HPLC (stationary phase: ISERA Metab-AAC column; mobile phase: 5 mM H_2SO_4 ; 0.6 mL min^{-1}) using an Agilent Refractive Index Detector (RID). Compounds in bioreactions were then quantified by relating the RID signal to the calibration curves (0.1 to 50 g L^{-1}) recorded with commercially available stan-

dards (glucose 100 000 RID_(10.4 min) = 0.75 g L^{-1} ; pyruvate 100 000 RID_(11.5 min) = 0.61 g L^{-1} ; lactate 100 000 RID_(13.2 min) = 0.53 g L^{-1} ; acetate 100 000 RID_(15.6 min) = 0.23 g L^{-1}). For analysis for indole, anthranilate, shikimate, chorismate, and indole-3-glycerol phosphate, supernatants (5 μL) were analysed by HPLC (stationary phase: Supersil AQ-C18, 5 μm , ID 4.6 mm \times 150 mm HPLC; mobile phase: $\text{H}_2\text{O}/\text{MeCN}$ 80:20 + 0.1% TFA; 1 mL min^{-1}) using UV-Vis detection (Agilent UV Detector; chorismate_(275 nm) 1000 AI_(6.1 min) = 0.98 g L^{-1} ; shikimate_(212 nm) 1000 AI_(9.3 min) = 1.07 g L^{-1} ; anthranilate_(254 nm) 1000 AI_(7.0 min) = 0.55 g L^{-1} ; indole_(280 nm) 1000 AI_(8.3 min) = 4.6 g L^{-1} ; indole-3-glycerol phosphate not detectable). Amino acids were quantified from clarified culture samples (as described above) by derivatization for 1 hour with 1:9 parts of OPA solution (*o*-phthalaldehyde and 3-mercaptopropionic acid solution in 0.4 M borate buffer, Agilent 5061-3335). An aliquot of the mixture (5 μL) was separated by HPLC (stationary phase: Supersil AQ-C18, 5 μm , ID 4.6 mm \times 150 mm; mobile phase: gradient at 40 °C with $\text{H}_2\text{O}/\text{MeCN}$ + 0.1% TFA (38% MeCN isocratic for 3 min, to 60% in 3 min, 60% isocratic for 1.5 min); 1 mL min^{-1}) and substances were quantified by UV compared to calibration curves (0.01 to 1 g L^{-1}) recorded with standards (tyrosine_(338 nm) 1000 AI_(3.5 min) = 1.92 g L^{-1} ; tryptophan_(338 nm) 1000 AI_(6.3 min) = 2.27 g L^{-1} ; phenylalanine_(338 nm) 1000 AI_(6.7 min) = 1.35 g L^{-1}).

Indigo quantification

Indigo content in the fermentation broth was determined by UV-visible spectroscopy at 610 nm after mixing of 50 μL well-resuspended broth with 950 μL of dimethylsulfoxide (DMSO). All indigo particles were solubilized by intense mixing and then the absorbance at 610 nm measured and related to a calibration curve (0.01 to 0.1 g L^{-1}) fitted with commercial 99.8% pure indigo standards ($\epsilon_{610 \text{ nm}}$ = 86.7 L g_{Indigo}⁻¹). Depending on the indigo concentration in the samples, additional dilutions were performed to ensure readout in the absorbance range of 0.2 to 0.8. Dry indigo purity was determined by weighting of a known amount of dry sample, dissolving it in DMSO to a known concentration (typically 10.0 mg in 50 mL).

Purification

At the end of the 0.5 L fermentations, the broth (*ca.* 0.7 L) was transferred into a 1 L Schott flask and left at room temperature without agitation allowing the indigo particles to sediment (3 to 5 hours at RT, Fig. 2B). Afterwards, the cell-containing top phase was removed by decanting, while the bottom phase (predominantly comprised of wet indigo) was kept. The indigo sediment was washed in three repetitive cycles of resuspension in water (2% w/v), sedimentation (5 to 8 hours at RT) and decanting of the top phase to finally give a crude indigo of purity of 70% (about 200 mg of wet indigo were isolated and dried at 60 °C for 48 hours to evaluate the purity after sedimentation).

The wet indigo paste was then resuspended in a solution of 0.5% w/v of citric acid and heated by autoclaving for



20 minutes at 121 °C. Once the liquor cooled to room temperature, the indigo was resuspended and filtered out (sintered glass filter grade 5). The isolated indigo cake was washed thoroughly with water (5 cake volumes) and dried at 60 °C for 48 hours. During the protocol development, HCl and H₂SO₄ at different concentrations (4 to 10%) were tested on the wet indigo isolated after sedimentation and washing and treated as described for the citric acid strategy. For the “leucoindigo” procedure, the wet indigo was treated with 1:5 w/w N₂S₂O₄ and 1:2 w/w NaOH for 1 hour under stirring in a sealed environment for the complete reduction of indigo to leucoindigo. The mixture was then filtered on a sintered glass (porosity 5), neutralised to pH 7 with Na₂CO₃ (solution 50%) and re-oxidised for 3 hours by bubbling of air through. Afterwards, the precipitated indigo was isolated by filtration, washed thoroughly with water (5 cake volumes) and dried at 60 °C for 48 hours.

Cotton fibres dyeing experiments and aromatic amines quantification

Those experiments were performed externally in an Archroma AG quality control (QC) laboratory in single-blind tests. Neither raw data nor methods details were reported to us.

Conclusions

In conclusion, we successfully engineered a robust *E. coli* strain (G5) to produce indigo from the renewable starting material glucose without leaving traces toxic anilines or other substances in the dye. This was achieved by introducing a unique combination of genetic modifications: the final strain expressed three mutated proteins from and had four promoters exchanged in the genome of *E. coli* BL21(DE3); additionally, four enzymes (NDOb, BX1, IH, and TnaA) were expressed from three plasmids in the final production strain G5.

Remarkably, the utilization of AhpC significantly enhanced cell robustness (*i.e.*, fermentations could be run for >70 hours with stable production profile and without uncontrollable foaming events), hence suggesting that mitigation of the oxidative stress due to NDOb catalysis and the formation of radical oxygen species is one of the key factors granting for process stability. Additionally, the isolation and utilization of naphthalene dioxygenase from *P. balearica* DSM 6083 (NDOb), was instrumental. Through this novel engineering approach and subsequent optimization of fermentation parameters and media, we attained a production titre of 12 g L⁻¹ of indigo, obtained in a fed-batch cultivation over 96 hours and with a yield $Y_{\text{indigo/glucose}} = 0.03 \text{ mole}_{\text{indigo}} \text{ mole}_{\text{glucose}}^{-1}$ (max theoretical $Y_{\text{indigo/glucose}} = 0.21 \text{ mole}_{\text{indigo}} \text{ mole}_{\text{glucose}}^{-1}$). Finally, a particularly interesting aspect is the development of a sustainable purification method, which exploits a minimal quantity of an environmentally friendly acid, validated through dyeing experiments on cotton fibres. The microbially produced indigo demonstrated excellent performance, comparable to its chemi-

cally produced counterpart but with undetectable traces of aromatic amines.

Clearly, many details of strain and process design have not yet reached their final stage. For example, strain G5 is still carrying 3 plasmids and the cultivation medium still contains complex components. However, it should be noted that the overall concept as demonstrated here seems valid, as we could transfer the optimized protocol for strain G5 directly to 500 L pilot scale, yielding 5 kg of dry indigo powder with approximately 80% purity (data shown in ESI figure, Fig. S12†). Given the intrinsic absence of toxic residues from chemical processes, the comparable performance during application, and the efficiency of the biological production process, we propose naming the produced material “bio-indigo” to reflect its sustainable microbial origin.

Author contributions

MP, TK, and MH conceptualized all the experiments; MP, LC, and TK performed the strain engineering and fermentation experiments; MP and MH developed the DSP methodology; MP performed the 500 L-scale pilot experiment; MP and MH curated data and wrote the manuscript; SP supervised the project; all the authors contributed to reviewing and editing the manuscript.

Data availability

The data supporting this article have been included as part of the ESI.† Furthermore, raw data including fermentation data are available at ETH Zurich repository, <https://www.research-collection.ethz.ch>.

Conflicts of interest

The authors declare that they have no competing interests.

Acknowledgements

We thank Innosuisse (Swiss Innovation Agency) for financial support (35973.1 IP-ENG). We thank Dr Maïke Otto (ETH Zurich) for supporting the project in the early stage. We thank Dr Maximilian Bahls (ETH Zurich), and Prof. Jochen Schmid (University of Munster, DE) for supporting the 500L-scale cultivation. We thank Archroma AG and Umberto De Vita for initializing and supporting the project, and for conducting QC and dyeing assessment.

References

- 1 H. Schmidt, *Chem. Unserer Zeit*, 1982, **16**, 57–67.



- 2 J. A. Linke, A. Rayat and J. M. Ward, *Bioresour. Bioprocess.*, 2023, **10**, 20.
- 3 R. Kohlhaupt and U. Bergmann, *US Pat*, 5116997, 1992.
- 4 R. Kohlhaupt, *US Pat*, 5424453, 1993.
- 5 Q. Pan, M. Held and J. Backmann, *RSC Sustain.*, 2025, **3**, 64–80.
- 6 N. Chandel, B. B. Singh, C. Dureja, Y. H. Yang and S. K. Bhatia, *World J. Microbiol. Biotechnol.*, 2024, **40**, 62.
- 7 K.-Y. Choi, *Dyes Pigm.*, 2020, **181**, 108570.
- 8 A. Berry, T. Dodge, M. Pepsin and W. Weyler, *J. Ind. Microbiol. Biotechnol.*, 2002, **28**, 127–133.
- 9 W. Weyler, T. C. Dodge, J. J. Lauff and D. J. Wendt, *US Pat*, 5866396, 1999.
- 10 T. Jakociūnas, M. K. Jensen and J. D. Keasling, *Metab. Eng.*, 2016, **34**, 44–59.
- 11 H. Shimizu and Y. Toya, *J. Biosci. Bioeng.*, 2021, **132**, 429–436.
- 12 N. N. Pham, Y. H. Wu, T. A. Dai, J. Tu, R. M. Liang, H. Y. Hsieh, C. W. Chang and Y. C. Hu, *Metab. Eng.*, 2024, **85**, 14–25.
- 13 Y. Yuk, J. H. Jang, S. A. Park, H. A. Park, J. O. Ahn, Y. H. Yang, S. Ham, S. H. Park, K. Park, S. Y. Kim, Y. S. Kim, J. Lee, U. J. Lee, B. G. Kim and K. Y. Choi, *Dyes Pigm.*, 2023, **218**, 111466.
- 14 L. Liu, M. Bilal, H. Luo, Y. Zhao and H. M. N. Iqbal, *Processes*, 2019, **7**, 213.
- 15 Y.-M. Ger, S.-L. Chen, H.-J. Chiang and D. Shiuan, *J. Biol. Chem.*, 1994, **269**, 5088–5093.
- 16 M. G. Caligiuri and R. Bauerle, *Science*, 1991, **252**, 1845–1848.
- 17 Y. Jiang, B. Chen, C. Duan, B. Sun, J. Yang and S. Yang, *Appl. Environ. Microbiol.*, 2015, **81**, 2506–2514.
- 18 L. Ferrer, M. Mindt, M. Suarez-Diez, T. Jilg, M. Zagorščak, J. H. Lee, K. Gruden, V. F. Wendisch and K. Cankar, *J. Agric. Food Chem.*, 2022, **70**, 5634–5645.
- 19 T.-H. Kim, S. Namgoong, J. H. Kwak, S.-Y. Lee and H.-S. Lee, *J. Microbiol. Biotechnol.*, 2000, **10**, 789–796.
- 20 K. Schroer, M. Kittelmann and S. Lütz, *Biotechnol. Bioeng.*, 2010, **107**, 321–329.
- 21 Y. Wang, H. Wang, L. Wei, S. Li, L. Liu and X. Wang, *Nucleic Acids Res.*, 2020, **48**, 6403–6412.
- 22 P. V. Dip, N. Kamariah, W. Nartey, C. Beushausen, V. A. Kostyuchenko, T. S. Ng, S. M. Lok, W. G. Saw, F. Eisenhaber, B. Eisenhaber and G. Grüber, *Biochim. Biophys. Acta, Bioenerg.*, 2014, **1837**, 1932–1943.
- 23 S. Pinhal, D. Ropers, J. Geiselmann and H. de Jong, *J. Bacteriol.*, 2019, **201**, e00047–e00019.
- 24 L. Liu, X. Duan and J. Wu, *PLoS One*, 2016, **11**, e0158200.
- 25 C. Kaleta, S. Schäuble, U. Rinas and S. Schuster, *Biotechnol. J.*, 2013, **8**, 1105–1114.
- 26 K. Gottlieb, C. Albermann and G. A. Sprenger, *Microb. Cell Fact.*, 2014, **13**, 1–16.
- 27 Y. Chen, Y. Liu, D. Ding, L. Cong and D. Zhang, *J. Ind. Microbiol. Biotechnol.*, 2018, **45**, 357–367.
- 28 P. B. Tayade and R. V. Adivarekar, *Fashion Textiles*, 2014, **1**, 1–16.
- 29 N. L. Saginaw, *US Pat*, 2159930, 1939.
- 30 E. Kupfer, *EP Pat*, 0730034A1, 1996.
- 31 W. Bretzel, W. Schurter, B. Ludwig, E. Kupfer, S. Doswald, M. Pfister and A. P. G. M. van Loon, *J. Ind. Microbiol. Biotechnol.*, 1999, **22**, 19–26.
- 32 M. R. Luo, *Color Res. Appl.*, 1981, **6**, 166–170.
- 33 G. Gibson, L. Young, R. Y. Chuang, J. C. Venter, C. A. Hutchison and H. O. Smith, *Nat. Methods*, 2009, **6**, 343–345.
- 34 A. Varma, B. W. Boesch and B. O. Paisson, *Biotechnol. Bioeng.*, 1993, **42**, 59–73.
- 35 B. Xiong, Y. Zhu, D. Tian, S. Jiang, X. Fan, Q. Ma, H. Wu and X. Xie, *Biotechnol. Bioeng.*, 2021, **118**, 1393–1404.

